Intrafibrillar Collagen Mineralization Produced by Biomimetic Hierarchical Nanoapatite Assembly

Yan Liu[Dr]
Department of Stomatology Tongji Hospital Tongji Medical College Huazhong University of Science and Technology, Wuhan, China

Nan Li[Dr]
College of Osteopedics & Traumatology Fujian University of Traditional Chinese Medicine, Fujian, China

Yi-pin Qi[Dr]
Department of Operative Dentistry and Endodontics Guanghua School of Stomatology Sun Yat-sen University, Guangzhou, China

Lin Dai[Dr]
Department of Stomatology The First Hospital of Wuhan, Wuhan, China

Thomas E. Bryan
Departments of Oral Biology and Endodontics School of Dentistry Medical College of Georgia, Augusta, Georgia, USA

Jing Mao[Dr]
Department of Stomatology Tongji Hospital Tongji Medical College Huazhong University of Science and Technology, Wuhan, China

David H. Pashley[Dr] and **Franklin R. Tay[Dr]**
Departments of Oral Biology and Endodontics School of Dentistry Medical College of Georgia, Augusta, Georgia, USA

Biomineralization templated by non-collagenous proteins is an example how nature uses nanotechnology to strengthen the load-bearing skeletons of vertebrates.[1–3] Mineralized collagen fibrils are responsible for the second level of hierarchy of bone structure[4] and account for its strength and toughness.[5] Calcium-deficient apatites are deposited in nanocrystalline form at the intrafibrillar and extrafibrillar spaces associated with the collagen fibrillar assembly.[6] Regulation of calcium phosphate phases during biomineralization is believed to exhibit two major characteristics.[7–9] The first is the sequestration of the calcium and phosphate ions into nanoscopic entities known as amorphous calcium phosphate (ACP). The second is the templating of mineral nucleation and growth through noncollagenous extracellular matrix proteins. These protein molecules contain polyanionic domains that are rich in polycarboxylic acid and phosphate function groups that bind to the collagen substrates at specific sites such as the gap zones of the collagen molecular assembly.[1,10] The immobilized proteins contain anionic charge sites wherein calcium binding and apatite nucleation occur at the aforementioned intrafibrillar locations. As a highly ordered manner of intrafibrillar mineralization at the nanoscale is responsible for the biomechanical properties of mineralized collagen,[11] this intricate

tayfranklin7@gmail.com .

biological process has inspired scientists to mimic its mechanism for creating mineralized type I collagen scaffolds to repair existing bone defects and/or generate new bone. Here, we demonstrate that the use of two phosphate-based templating analogs of matrix proteins in the presence of a polycarboxylic acid sequestration analog of ACPs results in a highly ordered intrafibrillar nanoapatite assembly that recapitulates the gap and overlap arrangement of collagen molecules within a collagen fibril. Adoption of a dual analog biomimetic strategy provides a means to produce advanced mineralized collagen scaffolds for tissue engineering applications.

Synthesis of collagen–apatite composites with chemical compositions similar to natural bone has been studied intensively in the last two decades because of interest in potential bone substitutes.[12–23] These studies have successfully demonstrated deposition of calcium phosphate minerals within a collagen matrix and contributed significantly to the understanding of biomimetic collagen mineralization. Nevertheless, the ability to replicate the intricate patterns of the nanocrystalline assembly at the intrafibrillar level has been elusive. As the contribution of amorphous mineral phases in hard tissue mineralization becomes firmly established,[24,25] more recent studies have successfully demonstrated intrafibrillar mineralization of collagen fibrils with polyaspartic acid-stabilized ACP nanophases.[26–30] This process is conceived to occur via a non-classical, particle-mediated mineralization mechanism[31] that involves infiltration of fluidic polymer-induced liquid precursors of ACP nanodroplets into the intrafibrillar compartments of a collagen fibril.[32] The nanodroplets fill the gap zones and microfibrillar spaces between the collagen molecules and eventually undergo phase transformation into a calcium-deficient apatite.[33] Although intrafibrillar mineralization of collagen fibrils with apatite has been elegantly demonstrated using polyaspartic acid as a biomimetic analog, biochemistry studies on extracellular matrix proteins involved in biomineralization of human hard tissues such as dentin matrix protein-1 demonstrate the dual sequestration and templating functional roles contributed by specific domains of these protein molecules.[8,9] It is not known if a biomimetic strategy that employs two biomimetic analogs to mimic matrix-bound non-collagenous proteins (i.e., one containing polycarboxylic acid groups and the other containing polyphosphonate or polyphosphate groups) confers any alteration in the ultrastructural characteristics of intrafibrillar mineralization when compared with the use of polycarboxylic acid alone for collagen mineralization.

Polyvinylphosphonic acid (PVPA) is a phosphonic acid containing polyanionic electrolyte that has been employed as a biomimetic analog of matrix phosphoproteins.[34,35] Sodium trimetaphosphate (STMP) is a chemical phosphorylation agent for food proteins and has been used with a variable degree of success in demonstrating precipitation of large spherulitic apatite clusters in the vicinity of a collagen matrix[36] and extrafibrillar mineralization of collagen.[37] By using polyacrylic acid (PAA) as the ACP sequestration analog and immobilization of either PVPA or STMP within collagen, we previously demonstrated initial evidence of hierarchical intrafibrillar nanoapatite assembly after 24 h of collagen mineralization.[38,39] The binding characteristics of these two molecules to type I collagen has been previously characterized using adsorption and desorption isotherms,from which the optimal concentrations employed in the present study were determined.[38,39] Although immobilization of PVPA relies on the size-exclusion characteristics[40] of cross-linked collagen to retain the templating molecules within the intrafibrillar compartments, immobilization of STMP appears to be achieved via chemical phosphorylation.[36,37] As the immobilization mechanisms of the two templating analogs are considerably different, the objective of the present work was to examine if one analog produces more efficient intrafibrillar collagen mineralization than the other.

In natural bone, collagen fibrils are produced by self-assembly of collagen molecules into fibrils prior to nucleation and growth of apatite crystallites (i.e., first level of structural hierarchy).[4] In the present work, a single-layer type I collagen was first reconstituted to serve as a scaffold for subsequent intrafibrillar deposition of apatite nanoplatelets. PVPA or STMP was then immobilized within the reconstituted collagen fibrils prior to mineralization. We examined the effects of PVPA and STMP on the second level of hierarchy of bone formation (i.e., mineralized collagen fibril level) by incorporating PAA as the sequestration analog in the mineralization medium. Transmission electron microscopy (TEM) was used to produce standardized low-magnification images of the grid spaces within individual TEM grids. A four-point scoring system with I: 0–25% mineralized (Figure 1 A); II: 26–50%; mineralized (Figure 1 B); III: 51–75% mineralized (Figure 1 C); and IV: 76–100% mineralized (Figure 1 D) was employed to evaluate the extent of matrix mineralization within the grid spaces of 24 grids derived from each of the two experimental groups. Only intrafibrillar mineralization of collagen fibrils was scored; extrafibrillar mineralization of the supporting carbon film (see Figures 1 C,D) was not included in the evaluation. For PVPA, the number of grids with median scores of I, II, III, and IV was 3, 6, 6, and 9, respectively. For STMP, the number of grids with median scores of I, II, III, and IV was 1, 5, 5, and 13, respectively (Supporting Information, Figure 1). Statistical analysis showed that there is no difference in the ability of the two templating analogs to induce intrafibrillar mineralization ($p = 0.214$, where the p-value is a measure of how much evidence one has against a null hypothesis of no effect. The smaller the p-value, the more evidence one has against the null hypothesis).

During the initial stage of intrafibrillar mineralization (4–8 h), collagen fibrils that eventually exhibited crystalline intrafibrillar minerals were infiltrated by an electron-dense amorphous mineral phase and appeared swollen (Supporting Information, Figure 2). The swollen fibrils measured 300–500 nm along their lateral dimensions when compared with the less electron-dense, nonswollen fibrils (ca. 50–200 nm in diameter) within the same grid space. For both the experimental groups and the control group (mineralization conduced with PAA only), the swollen appearance disappeared after 72 h as the amorphous mineral phased were transformed into electron-dense intrafibrillar minerals. Collagen fibrils are highly ordered in the axial dimension but relatively disordered in the lateral dimension;[41] lateral swelling of the fibrils occurs by water imbibition associated with pH changes and alterations in ionic strength.[42] Such a phenomenon probably occurs with fibrils that are lightly cross-linked with carbodiimide (see Experimental Section) and may not be seen in matrices that are cross-linked with glutaraldehyde. The temporary increase in lateral spacings of the collagen fibrils during the initial mineralization stage probably represents the results of infiltration of fluid-like ACP nanoprecursors via a polymer-induced liquid precursor process.[26,33] This lateral expansion might have resulted from the higher content of structural water within the intercluster spaces of ACPs.[43] Upon amorphous-to-crystalline transformation, excess water is progressively removed during the deposition of the apatite phase within the microfibrillar spaces or gap zones.[28] This progressive dehydration process might have resulted in the collagen fibrils resuming their original dimensions after mineralization was accomplished.

Intrafibrillar mineralization could be identified from the PAA control (Supporting Information, Figure 3A). The mineral phase consisted of arrays of mineral strands that were aligned with the collagen fibril's longitudinal axis (Supporting Information, Figure 3B). They also exhibited spiral surface features that resemble the rope-like microfibrillar substructure of unmineralized fibrils.[44] Selected area electron diffraction of those intact mineralized fibrils produced continuous ring patterns that are characteristic of the diffraction planes of polycrystalline apatite (Supporting Information, Figure 3C). The presence of partially unraveled mineralized microfibrils along the periphery of some fibrils allows the

ultrastructure of the intrafibrillar mineral to be more clearly discerned (Supporting Information, Figure 3D). Those unraveled strands appear to be continuous and discrete crystalline platelet morphology cannot be identified (Supporting Information, Figure 3E).

When collagen was mineralized in the presence of PAA as the ACP stabilization analog and PVPA or STMP as the templating analog, cross-banding created by overlapping apatite nanoplate-lets could be identified from the less heavily mineralized fibrils (Figure 2 A,C). As the mineralized collagen fibrils were examined en masse without sectioning, this 64-nm repeat (67-nm when hydrated) became obliterated by the denser minerals present in the heavily mineralized fibrils, a phenomenon that was also observed in small angle X-ray scattering as a reduced number of meridional reflections.[45] Cross-banding was more difficult to identify in the PVPA group because it was partially obscured by the mineralization of the supporting carbon film that was probably caused by PVPA binding to the carbon film (Figures 2 A,B). This form of non-specific PVPA binding was also seen in other applications of the polyanionic molecule.[46] High magnifications of mineralized fibrils from the STMP group revealed discrete mineral nanoplatelets (Figure 2 D) that were more heavily stacked along the gap zones of the fibrillar assembly to produce cross-banding patterns (Figure 2 E). Selected area electron diffraction of those fibrils resulted in arcshaped patterns along the (002) diffraction plane that is indicative of a highly hierarchical alignment of the C-axes of apatite nanoplatelets with the longitudinal axis of the mineralized fibril (Figure 2 F).

Hierarchical arrangement of discrete apatite nanoplatelets within the intrafibrillar spaces in the PVPA or STMP experimental group appears to be attributed to the binding of these molecules to the collagen fibrils. This is demonstrated by the appearance of phosphate-related peaks the infrared spectra recorded using Fourier transform infrared spectroscopy after unmineralized collagen matrices were treated with these templating analogs (Figure 3). Presumably, binding of these templating analogs to collagen allows the PAA-stabilized ACP nanoprecursors to be directed to specific locations such as the gap zones, where apatite nucleation occurs. In their absence, intrafibrillar mineralization also occurs when PAA is used alone to stabilize ACPs as nanoprecursors. The appearance of continuous intrafibrillar strands in the PAA control group suggests that the ACP nanoprecursors are capable of completely filling the microfibrillar spaces. The coalesced ACP phase may have been crystallized as a single entity instead of being templated into discrete nanoplatelets.

We also made preliminary investigations on the use of STMP for mineralization of thin 3D collagen scaffolds. This was achieved by reconstituting a 3 mg mL $^{-1}$ collagen solution on polylysine-coated cover slips. The matrices were examined by scanning electron microscopy. The results are summarized in the Supporting Information, Figure 4. The ability of a thicker fibrillar matrix to be mineralized confirms that a mineralized 3D scaffold may be mineralized using the dual functional motif-based biomimetic mineralization strategy. Observation of extrafibrillar mineralization along the surface of the mineralized fibrils (Supporting Information, Figure 4B,E) further supports that within a dense 3D scaffold, the intrafibrillarly mineralized fibrils will be bridged by extrafibrillar minerals in a manner that is analogous to the organization in naturally mineralized tissues.

Biomimetic mineralization of reconstituted collagen using dual biomimetic analogs successfully demonstrates the firsttwo hierarchical levels in natural bone. Collagen sponges saturated with recombinant human bone morphogenic protein-2 (BMP-2) have been used for localized delivery of osetoinductive signaling molecules for bone regeneration and fracture repair. However, non-mineralized collagen is a relatively ineffective vehicle for delivering BMP-2 as the latter binds poorly to collagen.[47] Thus, hierarchical assembly of nanoapatite within type I collagen appears to be a logical step toward creating biomimetic scaffolds for

delivery of these signaling molecules.[48] Mineralized collagen scaffolds with a denser arrangement of collagen fibrils than collagen sponges may provide mechanical support in load-bearing regions and the potential as a vehicle for sustained release of signaling molecules for stem cell commitment and cytodifferentiation.[49] They possess better osteoconductive properties and exhibit higher levels of osteogenic gene expression than nonmineralized polymeric scaffolds.[50] It may be possible to saturate collagen scaffolds with signaling molecules and fossilize these molecules within the mineralized matrix for their controlled release.

In summary, highly hierarchical intrafibrillar apatite nanocrystals can be assembled within reconstituted type I collagen fibrils using a biomimetic approach that involves the synchronized supplement of sequestration and templating biomimetic analogs during the mineralization process. Between the two templating analogs of matrix phoproteins, STMP is more economical and involves a simpler procedure for phosphorylating collagen for biomineralization purposes. With the application of this analog to more densely packed collagen scaffolds, biomimetically mineralized collagen matrices with hierarchical intrafibrillar apatite assembly may be produced that exhibit better load-bearing properties during function when compared to the use of non-mineralized polymeric scaffolds. This hypothesis should be tested in the future using biomechanic approaches such as conventional or nanoscopical dynamic mechanical analyses. Future research should also be directed toward investigating the potential of using these hierarchically mineralized collagen scaffolds as a means of delivering growth factors in bone and dentin regeneration.

Experimental Section

Self-Assembly of Collagen Fibrils

A single-layer of type I collagen fibrils was reconstituted over 400-mesh formvar-and-carbon-coated Ni TEM grids by neutralizing a 0.15 mg mL^{-1} collagen stock solution with ammonia vapor for 4 h. For preparation of collagen stock solution, lyophilized type I collagen powder derived from bovine skin (Sigma-Aldrich, St. Louis, MO, USA) was dissolved in 0.1 M acetic acid (pH 3.0) at 4 °C. The neutralized collagen solution was allowed to gel by incubation at 37 °C for 3–5 days.

Immobilization of Matrix Protein Analogs

For PVPA (M_w = 24 000, Polysciences, Inc., Warrington. PA, USA), a cross-linking procedure was used to stabilize the structure of the reconstituted collagen fibrils and to trap the PVPA molecules within the cross-linked collagen. This was performed by adding 500 μg mL^{-1} PVPA to 0.3 M 1-ethyl-3-(3-dimethylaminopropyl)-carbodiimide (EDC)/0.06 M N-hydroxysuccinimide (NHS) (ThermoScientific Pierce, Rockford, IL, USA) and adjusting the pH to 5.5 with 0.1 M 2-morpholinoethane sulphonic acid buffer. The collagen grids were treated at ambient temperature for 4 h. Being a zero-length cross-linking agent, EDC couples carboxyl groups to primary amines between collagen molecules without introducing extrinsic material between the two moieties. The PVPA has a molecular mass of 24 kDa and is a mixture of PVPA polymers that include some that are smaller and larger than 24 kDa. By cross-linking collagen with EDC, the sieving properties of collagen were increased for trapping PVPA within collagen.[40] For STMP (M_w = 367.9, Sigma-Aldrich), the reconstituted collagen was first cross-linked with EDC and NHS as described previously but without inclusion of PVPA. As protein phosphorylation with STMP is usually performed at pH > 11 to open its closed ring structure via alkaline hydrolysis,[51] 2.5 wt% STMP was hydrolyzed at pH 12 for 5 h followed by neutralization to pH 7.4 before it was used for treating the cross-linked reconstituted collagen for 1 h. Collagen-coated grids were

randomly treated with PVPA ($N = 24$, where N is the number of specimens) or STMP ($N = 24$) and air-dried.

Collagen Mineralization

A composite disk composed of a light-polymerizable hydrophilic resin blend, set white Portland cement powder, and silanized silica was used as calcium and hydroxyl ion releasing sources.[35] Simulated body fluid (SBF) was prepared by dissolving 136.8 m M NaCl, 4.2 m M NaHCO$_3$, 3.0 m M KCl, 1.0 m M K$_2$HPO$_4$·3H$_2$O, 1.5 m M MgCl$_2$·6H$_2$O, 2.5 m M CaCl$_2$, 0.5 m M Na$_2$SO$_4$,and 3.08 m M Na$_3$N in deionized water and used as the phosphate source. Polyacrylic acid (PAA, M_w = 1 800, Sigma-Aldrich) was added to SBF to stabilize amorphous calcium phosphate as a nanoprecursors.[34] For each nanoscopic mineralization assembly, the analog-bound grid was floated upside down on one 30 μL drop of SBF containing 1 000 μg mL^{-1} PAA placed on top of the composite disk and sealed inside a 100% humidity chamber.[35] Mineralization was first performed with additional grids for 4–8 h at 37 °C to examine the initial status of the collagen fibrils. After confirming that electron-dense mineral phase was present with the collagen fibrils, subsequent mineralization was all performed at 37° C for 72 h prior to examination by transmission electron microscopy (TEM). Control TEM grids consisting of cross-linked reconstituted collagen (without PVPA or STMP) were immersed in the composite–SBF assembly with the latter containing 1000 μg mL^{-1} PAA. After retrieval, each grid was dipped in and out of deionized water and examined unstained with a JEM-1230 TEM (JEOL, Tokyo, Japan) at 110 kV. Images were taken at low magnification (1 000×) for scoring the extent of collagen mineralization. Higher magnification images were taken for examination of the ultrastructural features of intrafibrillar mineralization. Selected area electron diffraction of mineralized fibrils was performed using centered dark-field imaging.

Statistical Analysis

The four-point scoring system (scores I–IV) described previously represented a continuous variation of the extent of collagen mineralization identified from each individual grid. For each TEM grid in each experimental group ($N = 24$), 10 grid spaces representing the most preponderant collagen mineralization results identified from that grid were scored. The median score was used to summarize the 10 scores taken from each grid. The Mann–Whitney rank sum test was used to evaluate those median scores to determine if the mineralization results in the two experimental groups were significantly different. Statistical significance was preset at $\alpha = 0.05$.

Fourier Transform Infrared Spectroscopy (FT-IR)

CollaCote (Zimmer, Carlsbad, CA, USA), a collagen wound dressing material prepared from purified type I bovine collagen, was used for characterization of the collagen matrix after treatment with PVPA or STMP. A Nicolet 6700 FT-IR spectrophotometer (ThermoScientific) with an attenuated total reflection setup was used to collect spectra from the collagen matrices after cross-linking and after treatment with the respective templating analog. Analog-treated collagen matrices were rinsed with deionized for 24 h and air-dried prior to FT-IR analysis. Additional spectra were collected from PVPA and STMP. Spectra were collected between 4,000–600 cm^{-1} at 4 cm^{-1} resolution using 32 scans. Data were normalized to the collagen amide I peak (1715–1596 cm^{-1})forcomparison.

Supplementary Material

Refer to Web version on PubMed Central for supplementary material.

Acknowledgments

References

[1]. Veis A. Rev. Mineral. Geochem. 2003; 54:249.

[2]. Weiner S, Nudelman F, Sone E, Zaslansky P, Addadi L. Biointerfaces. 2006; 1:P12.

[3]. George A, Ravindran S. Nano Today. 2010; 5:254. [PubMed: 20802848]

[4]. Weiner S, Traub W. FASEB J. 1992; 6:879. [PubMed: 1740237]

[5]. Gupta HS, Seto J, Wagermaier W, Zaslansky P, Boesecke P, Fratzl P. Proc. Natl. Acad. Sci. USA. 2006; 103:17741. [PubMed: 17095608]

[6]. Landis WJ, Hodgens KJ, Song MJ, Arena J, Kiyonaga S, Marko M, Owen C, McEwen BF. J. Struct. Biol. 1996; 117:24. [PubMed: 8776885]

[7]. He G, Dahl T, Veis A, George A. Nat. Mater. 2003; 2:552. [PubMed: 12872163]

[8]. He G, Gajjeraman S, Schultz D, Cookson D, Qin C, Butler WT, Hao J, George A. Biochemistry. 2005; 44:16140. [PubMed: 16331974]

[9]. Gajjeraman S, Narayanan K, Hao J, Qin C, George A. J. Biol. Chem. 2007; 282:1193. [PubMed: 17052984]

[10]. George A, Veis A. Chem. Rev. 2008; 108:4670. [PubMed: 18831570]

[11]. Gao H, Ji B, Jäger IL, Arzt E, Fratzl P. Proc. Natl. Acad. Sci. USA. 2003; 100:5597. [PubMed: 12732735]

[12]. Saito T, Arsenault AL, Yamauchi M, Kuboki Y, Crenshaw MA. Bone. 1997; 21:305. [PubMed: 9315333]

[13]. Bradt JH, Mertig M, Teresiak A, Pompe W. Chem. Mater. 1999; 11:2694.

[14]. Kikuchi M, Itoh S, Ichinose S, Shinomiya K, Tanaka J. Biomaterials. 2001; 22:1705. [PubMed: 11396873]

[15]. Rhee SH, Suetsugu Y, Tanaka J. Biomaterials. 2001; 22:2843. [PubMed: 11561889]

[16]. Tampieri A, Celloti G, Landi E, Sandri M, Roveri N, Falini GJ. J. Biomed. Mater. Res. 2003; 67:618. Part A.

[17]. Liao SS, Cui FZ, Zhang W, Feng QL, Q. L. J. Biomed. Mater. Res. 2004; 69B:158. Part B.

[18]. Girija EK, Yokogawa Y, Nagata F. J. Mater. Sci. Mater. Med. 2004; 15:593. [PubMed: 15386967]

[19]. Lickorish D, Ramshaw JAM, Werkmeister JA, Glattauer V, Howlett CR. J. Biomed. Mater. Res. 2004; 68:19. Part A.

[20]. Thomas V, Dean DR, Jose MV, Mathew B, Chowdhury S, Vohra YK. Biomacromolecules. 2007; 8:631. [PubMed: 17256900]

[21]. Sena LA, Caraballo MM, Rossi AM, Soares GA. J. Mater. Sci. Mater. Med. 2009; 20:2395. [PubMed: 19585226]

[22]. Liu C, Han Z, Czernuszka JT. Acta Biomater. 2009; 5:661. [PubMed: 18990616]

[23]. Nitzsche H, Lochmann A, Metz H, Hauser A, Syrowatka F, Hempel E, Müller T, Thurn-Albrecht T, Mäder K. J. Biomed. Mater. Res. 2010; 94:298. Part A.

[24]. Weiner S, Sagi I, Addadi L. Science. 2005; 309:1027. [PubMed: 16099970]

[25]. Mahamid J, Sharir A, Addadi L, Weiner S. Proc. Natl. Acad. Sci. USA. 2008; 105:12748. [PubMed: 18753619]

[26]. Olszta MJ, Cheng X, Jee SS, Kumar R, Kim YY, Kaufman MJ, Douglas EP, Gower LB. Mater. Sci. Eng. R. 2007; 58:77.

[27]. Deshpande AS, Beniash E. Cryst. Growth Des. 2008; 8:3084.

[28]. Chesnick IE, Mason JT, Giuseppetti AA, Eidelman N, Potter K. Biophys. J. 2008; 95:2017. [PubMed: 18487295]

[29]. Nassif N, Gobeaux F, Seto J, Belamie E, Davidson P, Panine P, Mosser G, Fratzl P, Giraud-Guille MM. Chem. Mater. 2010; 22:3307.

[30]. Jee SS, Thula TT, Gower LB. Acta Biomater. 2010; 6:3676. [PubMed: 20359554]

[31]. Xu AW, Ma Y, Cölfen H. J. Mater. Chem. 2007; 17:415.

[32]. Olszta MJ, Odom DJ, Douglas EP, Gower LB. Connect. Tissue Res. 2003; 44:326. [PubMed: 12952217]

[33]. Gower LB. Chem. Rev. 2008; 108:4551. [PubMed: 19006398]

[34]. Tay FR, Pashley DH. Biomaterials. 2008; 29:1127. [PubMed: 18022228]

[35]. Kim YK, Gu LS, Bryan TE, Kim JR, Chen L, Liu Y, Yoon JC, Breschi L, Pashley DH, Tay FR. Biomaterials. 2010; 31:6618. [PubMed: 20621767]

[36]. Li X, Chang J. J. Biomed. Mater. Res. 2008; 85:293.

[37]. Xu Z, Neoh KG, Kishen A. Mater. Sci. Eng. C. 2010; 30:822.

[38]. Gu LS, Kim YK, Liu Y, Takahashi K, Arun S, Wimmer CE, Osorio R, Ling JQ, Looney SW, Pashley DH, Tay FR. Acta Biomater. 2011; 7:268. [PubMed: 20688200]

[39]. Gu LS, Kim YK, Liu Y, Ryou H, Wimmer CE, Dai L, Arola DD, Looney SW, Pashley DH, Tay FR. J. Dent. Res. in press DOI:10.1177/0022034510385241.

[40]. Toroian D, Lim JE, Price PA. J. Biol. Chem. 2007; 282:22437. [PubMed: 17562713]

[41]. Hulmes DJS, Wess TJ, Prockop DJ, Fratzl P. Biophys. J. 1995; 68:1661. [PubMed: 7612808]

[42]. Svendsen KH, Koch MHJ. EMBO J. 1982; 1:669. [PubMed: 7188356]

[43]. Dorozhkin SV. Acta Biomater. 2010; 6:4457. [PubMed: 20609395]

[44]. Bozec L, Van Der Heijden G, Horton M. Biophys. J. 2007; 92:70. [PubMed: 17028135]

[45]. Burger C, Zhou H, Wing H, Sics I, Hsiao BS, Chu B, Graham L, Glimcher MJ. Biophys. J. 2008; 95:1985. [PubMed: 18359799]

[46]. Korlach J, Marks PJ, Cicero RL, Gray JL, Murphy DL, Roitman DB, Pham TT, Otto GA, Foquet M, Turner SW. Proc. Natl. Acad. Sci. USA. 2008; 105:1176. [PubMed: 18216253]

[47]. Laub M, Chatzinikolaidou M, Jennisen HP. Materialwiss. Werkst-offtech. 2007; 38:1019.

[48]. Fröhlich M, Grayson WL, Wan LQ, Marolt D, Drobnic M, Vunjak-Novakovic G. Curr. Stem Cell Res. Ther. 2008; 3:254. [PubMed: 19075755]

[49]. Hirano Y, Mooney DJ. Adv. Mater. 2004; 16:17.

[50]. Tsai SW, Hsu FY, Chen PL. Acta Biomater. 2008; 4:1332. [PubMed: 18468966]

[51]. Shen CY. Ind. Eng. Chem. Prod. Res. Dev. 1966; 5:272.

[52]. Wang XH, Li DP, Wang WJ, Feng QL, Cui FZ, Xu YX, Song XH, VanDerWerf M. Biomaterials. 2003; 24:3213. [PubMed: 12763448]
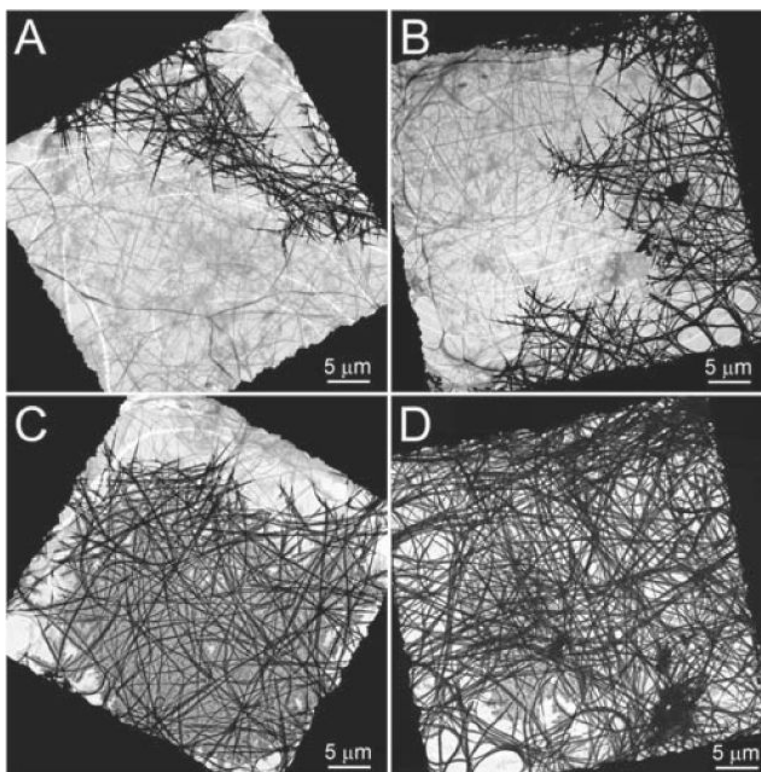
Figure 1.
A four-point scoring system for examining the extent of collagen mineralization within TEM grid spaces. A) 0–25% mineralization; B) 26–50% mineralization; C) 51–75% mineralization; D) 76–100% mineralization. Mineralized collagen fi brils appeared as highly electron-dense (black) fi brils. Extrafi brillar mineralization of the supporting carbon fi lm was not included in the evaluation.
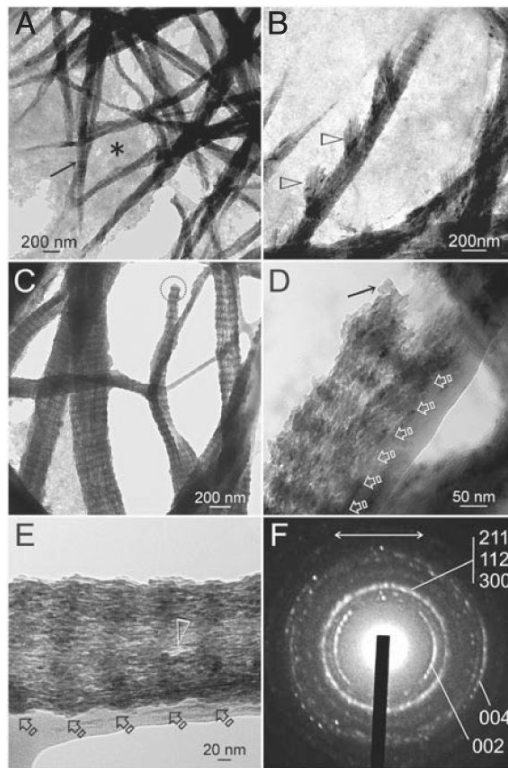
Figure 2.
Unstained TEM images of mineralized collagen retrieved after 72 h from the experimental groups in which mineralization was performed with immobilized PVPA or STMP and in the presence of polyacrylic acid in the mineralization medium. A) For the PVPA group, cross-bandings were more difficult to identify (arrow) as they were partially obscured by mineralization of the supporting carbon film (asterisk). B) High magnification of (A) showing hierarchical arrangement of intrafibrillar minerals, which gave rise to the appearance of cross-banding patterns along the fibril. Open arrowheads: extrafibrillar mineral deposits. C) For the STMP group, collagen banding was more easily recognized because there was less heavy mineralization of the supporting carbon film. The dotted circle highlights a fractured mineralized fibril (see also Supporting Information, Figure 3B,D). D) High magnification a fractured fibril similar to the one depicted in (C) exposing an intrafibrillar crystalline platelet (ca. 10 nm × 20 nm) along the fractured edge (arrow). Hierarchical arrangement of the nanocrystals resulted in a cross-banded appearance along the rest of the fibril (open arrows) E) A fibril imaged in a direction such that the intrafibrillar nanocrystals are oriented along their sides, producing a needle-shaped appearance of the nanocrystals. A denser packing of the nanocrystals at periodic sites (open arrows) along the fibril's lateral dimension resulted in a crystalline arrangement that corresponded with the *d*-spacing (ca. 64 nm) of the collagen fibril. A defect within the fibril (open arrowhead) reveals individual intrafibrillar nanocrystals. F) Selected area electron diffraction of the fibril shown in (E) indicates that the mineral phase is apatite. The (002) diffraction plane is arc-shaped and is oriented parallel to the longitudinal axis of the mineralized fibril (arrow). The (211), (112), and (300) diffraction planes are close to one another, producing a thicker and apparently continuous ring.
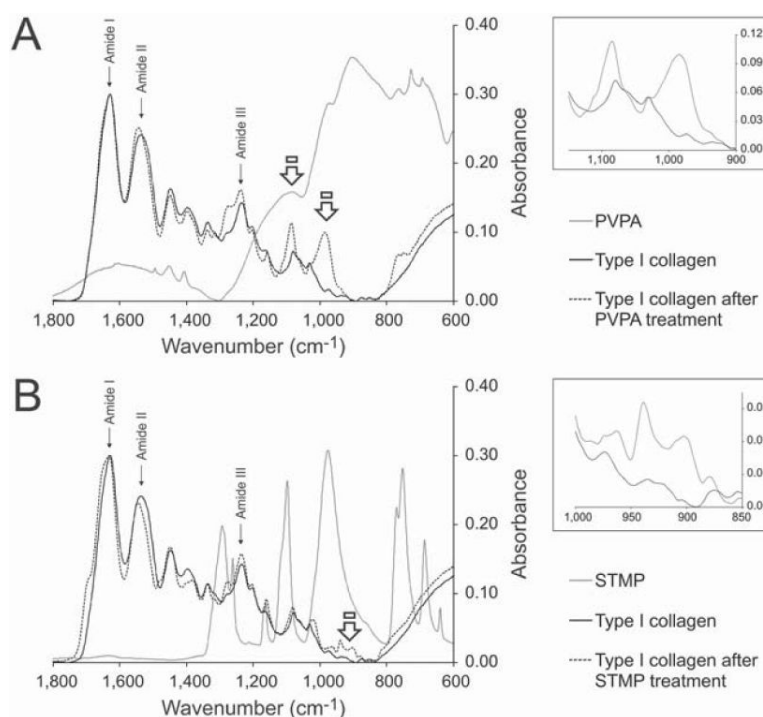
Figure 3.
A) Infrared spectra of PVPA (solid gray line), type I bovine collagen (CollaCote; solid black line), and type I collagen treated with 0.3 M 3-(3-dimethylaminopropyl)-carbodiimide (EDC)/0.06 M *N*-hydroxysuccinimide (NHS) cross-linking solution containing 500 µg mL^{-1} PVPA to trap the PVPA molecules within the collagen matrix (dotted black line). Spectral peaks of interest from 1 800–800 cm^{-1} are shown. The amide I, II, and III peaks are characteristic of type I collagen. The two collagen spectra were normalized against their amide I peaks. Changes in the amide II and III peaks (N–H bending vibrations coupled to C–N stretching vibrations) are associated with EDC cross-linking.[52] New phosphate peaks associated with immobilization of PVPA (open arrows) are shown at higher magnification in the right inset. B) Infrared spectra of STMP (solid gray line), type I collagen (solid black line), and type I collagen treated with 2.5 wt% STMP. New phosphate-associated peaks (open arrow) are shown at higher magnification in the right inset.